HHS Public Access

Author manuscript

Cancer Chemother Pharmacol. Author manuscript; available in PMC 2019 March 01.

Published in final edited form as:

Cancer Chemother Pharmacol. 2018 March ; 81(3): 483–495. doi:10.1007/s00280-017-3509-0.

Combinatorial effects of histone deacetylase inhibitors (HDACi), vorinostat and entinostat, and adaphostin are characterized by distinct redox alterations

Nilsa Rivera-Del Valle[*], **Tiewei Cheng**[*], **Mary E. Irwin**, **Hayley Donnella**, **Melissa M. Singh**, and **Joya Chandra**

Department of Pediatrics Research, Children's Cancer Hospital; Center for Cancer Epigenetics, The University of Texas (UT) M. D. Anderson Cancer Center, Houston, TX 77030, U.S.A. (N.R.V, T.C. M.M.S, H.D., M.E.I, J.C.); Graduate School of Biomedical Sciences, UT Health Science Center at Houston and UT MD Anderson Cancer Center, Houston, TX 77030, U.S.A. (N.R.V., J.C.)

Abstract

Purpose—Amongst the epigenetically-targeted therapies, targeting of the histone deacetylases (HDACs) has yielded numerous drugs for clinical use in hematological malignancies, but none as yet for acute lymphocytic leukemia (ALL). Single agent activity of HDAC inhibitors (HDACi) has been elusive in ALL, and has prompted study of combinatorial strategies. Because several HDACi raise levels of intracellular oxidative stress, we evaluated combinations of two structurally distinct HDACi with the redox active compound adaphostin in acute lymphocytic leukemia (ALL).

Methods—The HDACi vorinostat and entinostat were tested in combination with adaphostin in human ALL cell lines. DNA fragmentation, caspase activation, mitochondrial disruption and levels intracellular peroxides, superoxide and glutathione were measured in cells treated with the HDACi/adaphostin combinations. Antioxidant blockade of cell death induction and gene expression profiling of cells treated with vorinostat/adaphostin versus entinostat/adaphostin combinations was evaluated.

Results—Both combinations synergistically induced apoptotic DNA fragmentation, which was preceded by an increase in superoxide levels, a reduction in mitochondrial membrane potential, and an increase in caspase-9 activation. The antioxidant N-acetylcysteine (NAC) blocked superoxide generation and prevented reduction of mitochondrial membrane potential. NAC decreased DNA fragmentation and caspase activity in cells treated with adaphostin and vorinostat, but not in those treated with adaphostin and entinostat. Gene expression arrays revealed differential regulation of several redox genes prior to cell death induction.

Corresponding author: Joya Chandra, Ph.D., Department of Pediatrics Research, The University of Texas M. D. Anderson Cancer Center, 1515 Holcombe Blvd. Unit 853 Houston TX, 77030, Phone: (713) 563-5405, Fax: (713) 404-6527, jchandra@mdanderson.org.

[*]Indicates equal contribution to manuscript.

Compliance with ethical standards:

Conflict of interest: All authors declare that he/she have no conflict of interest.

Ethical approval: This article does not contain any studies with human participants or animals performed by any of the authors.

Conclusions—A redox modulatory agent, adaphostin, enhances efficacy of two HDACi, vorinostat or entinostat, but via different mechanisms indicating a point of divergence in the mechanisms of synergy between the two distinct HDACi and adaphostin.

Keywords

HDAC; HDAC inhibitor; ROS; oxidative stress; ALL

1. Introduction

Histone deacetylase inhibitors (HDACi) are a structurally diverse class of drugs that inhibit enzymes in the eleven member HDAC family. Since HDACs deacetylate protein substrates including histones, the HDACi promote histone acetylation, chromatin relaxation, and re-expression of silenced genes [1] and also promote acetylation of non-histone protein which may or may not alter protein expression, function or localization. HDACi have been found induce cell cycle arrest, differentiation, and apoptosis of several cancer types, including hematological malignancies [2, 3]. Several HDACi are currently in clinical use for lymphoma and myeloma, with many clinical trials underway in both solid and liquid tumors. Efforts to integrate HDACi into chemotherapy regimens for high risk and relapsed acute lymphocytic leukemia (ALL) are ongoing and offer an opportunity to improve outcomes for these poor prognosis patients for whom the five year overall survival rate is only 50%.

Vorinostat, a hydroxamic acid derivative, was the first HDACi approved by the FDA to treat cutaneous T-cell lymphoma that is progressive, persistent, or recurrent after two systemic therapies [4]. Vorinostat inhibits class I, II, and IV HDACs, and is considered a pan HDACi [4]. Entinostat, a benzamide derivative, is a class I HDAC inhibitor and has been evaluated in Phase I and II clinical trials for the treatment of hematologic malignancies [5–7]. Preclinical studies have well documented that HDACi exert their anti-cancer effects through various mechanisms given the broad regulatory targets of HDACi [8]. One mechanism is to promote histone hyper-acetylation and consequentially reactivation of silenced genes regulating DNA repair, cell cycle arrest, and apoptosis [9]. It is also interesting to note that HDACi promote oxidative stress and generation of reactive oxygen species (ROS). For example, vorinostat triggers caspase-independent death of T-leukemia cells via ROS generation, which can be abrogated by pre-treatment with antioxidants [3]. Similarly, entinostat induces the intrinsic apoptosis pathway in myelomonocytic leukemia cells via increase of oxidative stress, and this apoptosis is abolished by pre-treatment with the antioxidant N-acetyl cysteine (NAC) [10].

Although vorinostat as a single agent has enjoyed some clinical success [11], researchers are testing combination therapies to enhance the efficacy of HDACi. One prominent example is the empirical preclinical and clinical testing of HDACi with conventional DNA damaging chemotherapeutics like doxorubicin, gemcitabine, and docetaxel with varying degrees of success.[12]. Some notable combinations are already in early phase I and/or II clinical trials. For example, the combination of vorinostat with azacitidine in patients with newly diagnosed acute myelogenous leukemia is being tested in a phase II clinical trial (NCT00948064). Another trial has evaluated vorinostat plus decitabine in patients with

relapsed/refractory AML in a phase I setting [13]. Several preclinical studies have shown that HDACi sensitize leukemia cells to the proteasome inhibitor [14], resveratrol [15] and the BCR/ABL kinase inhibitor KW-2449 [16] via an oxidative stress dependent cell death pathway. However, given that both vorinostat and entinostat promote ROS-dependent apoptosis in leukemia cells, little has been done to examine the possibility of enhancing HDACi efficacy by specifically augmenting ROS generation pharmacologically.

Adaphostin is the adamantyl derivative of a tyrphostin kinase inhibitor and has been proposed to be a potential anticancer drug for the treatment of acute leukemia, in part because it is selectively toxic to leukemia cells as compared to normal lymphocytes[17] [18]. In addition to inhibiting tyrosine kinase activity, adaphostin also promotes oxidative stress in cancer cells by several mechanisms, including binding directly to complex III of the electron transport chain and up-regulating the expression of several oxidative stress-related genes such as glutathione s-transferase, superoxide dismutase and heme oxygenase-1 [18–21].

Here, we hypothesized that increasing intracellular ROS levels using adaphostin would augment cytoxicity of distinct HDACi with different specificities. We demonstrated, for the first time, synergistic, cytotoxic effects of the combinations, which are accompanied by potentiation of ROS generation, mitochondrial disruption, and caspase activation. However, while adaphostin promotes cell death of both vorinostat and entinostat in acute leukemia lines, the synergy is characterized by redox gene alterations specific to the HDACi being used.

2. Material and Methods

Cell lines

Jurkat cells, a human T-Acute Lymphocytic Leukemia (T-ALL), and I9.2 (caspase-8 deficient Jurkat) cells were acquired from American Type Culture Collection (Manassas, VA). Molt-4 cells (T-ALL); were kindly provided by Dr. Patrick A. Zweidler-McKay (The University of Texas M.D. Anderson Cancer Center, Houston, TX). All cell lines were verified by STR DNA fingerprinting by the M.D. Anderson characterized cell line core (CCSG) laboratory. Cells were grown in a humidified incubator with 5% CO_2 at 37° C and cultured in RPMI 1640 with 10% (v/v) heat-inactivation fetal bovine serum (Hyclone, Logan, UT), 2 mM L-glutamine, 100 U/mL penicillin, and 100 μg/mL streptomycin (Sigma St. Louis, MO).

Chemicals and antibodies

Adaphostin was generously provided by Dr. Robert Shoemaker at the NCI/NIH Developmental Therapeutic Program (Bethesda, MD). Vorinostat was purchased from Cayman Chemicals (Ann Arbor, MI) and entinostat was kindly provided by Syndax Pharmaceuticals (Waltham, MA). Propidium iodide (PI) and N-acetyl cysteine (NAC) were purchased from Sigma (St. Louis, MO). Dye for the detection of intracellular superoxide (dihydroethium - HE) was purchased from Invitrogen (Grand Island, NY). Tetramethylrhodamine ethyl ester (TMRE) was purchased from Molecular Probes (Eugene,

OR). Caspase-3 substrate, DEVD-amc and the caspase inhibitors zVAD-fmk, DEVD-fmk, LEHD-fmk and IETD-fmk were purchased from Enzo Life Sciences (Farmingdale, NY).

DNA fragmentation and synergy analysis

The percentage of sub-diploid population was measured as an indicator of apoptosis using propidium iodide (PI) staining followed by flow cytometric analysis. After 24 h of incubation with desired treatment, cells were centrifuged, washed with PBS and suspended in 500 μL of PI solution (50 μg/mL PI, 0.1% Triton X-100, and 0.1% sodium citrate in PBS) for a minimum of 3 h. Samples were assessed by flow cytometry on the FL-3 channel (FACSCalibur, Becton, Dickinson, Franklin Lakes NJ). CellQuest software (BD Bioscience, Franklin Lakes NJ) was used for the analysis of the data. After three different experiments synergy was calculated using isobologram analysis based on the Chou and Talalay method [22] with Calcusyn software (Biosoft, Ferguson, MO).

Detection of changes in mitochondrial membrane potential

Changes in mitochondrial membrane potential were measured using tetramethylrhodamine ethyl ester (TMRE) staining. After treatment, cells were centrifuged, washed with PBS, and incubated with 25 nM TMRE in 10 mM HEPES, 150 mM NaCl, 5 mM KCl, 1 mM MgCl, and 1.8 mM CaCl, pH 7.4 in a volume of 1 mL for 30 min. at 37°C in the dark. After 30 min. cells were washed in PBS and fluorescence intensity was analyzed by flow cytometry on the FL-2 channel of a FACSCalibur flow cytometer and analyzed by CellQuest software (BD Bioscience, Franklin Lakes NJ).

Detection of intracellular superoxide

The intracellular superoxide level was measured using the cell-permeable dihydroethidium (HE) dye followed by flow cytometry analysis. Briefly, cells were centrifuged and suspended in 1 mL of PBS containing 10 μM HE. The samples were incubated for 30 min. in the dark at 37° C. After 30 min. incubation, cells were centrifuged and washed with PBS and suspended in 500 μl of PBS. Fluorescence intensity was assessed by flow cytometer on the FL-3 channel and analyzed by CellQuest software (BD Bioscience, Franklin Lakes NJ).

Caspase-3-like activity assays

After treatment, cells were centrifuged, washed with PBS and suspended in in 150 μl PBS, and lysed by freezing and thawing once in dry ice. Triplicates of 50 μl of lysate were loaded on a 96-well plate and 150 μl of 50 μM DEVD-amc in DEVD buffer (10% sucrose, 0.001% IGEPAL, 0.1% CHAPS, 5 mM HEPES, pH 7.25) were added to each well. The release of fluorescence (amc) generated from the cleavage of DEVD-amc was measured using a spectrofluorometer (SpectraMax Gemini EM, Molecular Devices, Sunnyvale, CA) using an excitation of 355 nm and emission of 460 nm.

Quantification of cellular glutathione (GSH) levels

After 24 h of treatment, cells were harvested and equal numbers of cells were aliquoted to new tubes and 50 μM of monochlorobromine was added to each sample, except for the unstained control. Cells were incubated with the dye for 15 minutes at 37°C. After

incubation, the reaction was stopped by adding trichloroacetic acid to a final concentration of 5%. Samples were collected and equal volume of methylene chloride was added. After samples were vortexed they were centrifuged at 3500 RPM for 2 minutes and 200 μl from the aqueous phase was collected in a well of a white opaque 96 well plate. Fluorescence was measured using a microplate reader (Spectra Gemini EM, Molecular Devices, Inc. Sunnyvale CA) with excitation 398 nm and emission of 488 nm. GSH level was calculated using a standard curve with increasing GSH concentration that was prepared in parallel with the samples.

Oxidative stress and antioxidant defense PCR array

Total RNA was isolated from cells using the RNeasy Mini Kit (Qiagen, Valencia, MA). The concentration and quality of the RNA were measured using a NanoDrop ND-1000 Spectrophotometer (Thermo Scientific Inc., Walthaman, MA). For each sample, 0.5 μg of RNA was used to synthesize cDNA. The synthesis of cDNA was performed using the RT^2 First Strand Kit (Qiagen, Valencia, MA). Real-time PCR was performed according to the manufacturer protocol for the RT^2 Profiler PCR array for Human Oxidative Stress and Antioxidant Defense (Qiagen, Valencia, MA).

Quantitative real time PCR

Total RNA was extracted from 2×10^6 Jurkat cells using the RNeasy Mini kit (QIAGEN, Valencia, CA) according to the manufacturer's protocol. cDNA was synthesized from 1 μg of RNA using iScript cDNA synthesis kit (Bio-Rad, Hercules, CA) according to the manufacturer's instructions. cDNA was diluted 1:5 and quantitative polymerase chain reaction (qPCR) was carried out using iTaq™ Universal SYBR® Green Supermix (Bio-Rad Laboratories, Hercules, CA), and either AOX-1 (Genecopoeia, Rockwille, MD). The annealing temperature for all PCR samples was 60°C, and the reaction was carried out for 40 cycles. Relative expression of genes of interest were analyzed by calculating the cycle threshold (Ct) values and normalized to actin Ct values.

Statistical analysis

For each condition, multiple experiments were performed, and the results are presented as the mean ± S.D. The differences between two group conditions were analyzed using independent, two-tailed *t*-tests (Microsoft Excel software, Redmond, WA).

3. Results

3.1 HDACi synergize with adaphostin to induce DNA fragmentation in ALL cells

As single agents, vorinostat, entinostat, and adaphostin show *in vitro* efficacy against leukemia cell lines via a mechanism that increases ROS production [3, 23, 24]. Because oxidative stress induces cell death, we sought to determine whether the ROS generating compound adaphostin would synergistically enhance vorinostat and entinostat-mediated leukemia cell death. Jurkat and Molt-4 cells were treated with increasing concentrations of vorinostat or entinostat alone or in combination with adaphostin for 24 hours, and DNA fragmentation was measured by flow cytometry following propidium iodide staining.

Treatment of Jurkat and Molt-4 cells with adaphostin, vorinostat, and entinostat as single agents induced DNA fragmentation compared to untreated control cells (Figure 1A–B). Further, treating these cells with adaphostin-vorinostat or adaphostin-entinostat combinations significantly enhanced DNA fragmentation compared to single agents alone (Figure 1A–B). Isobologram analysis using the Chou and Talalay method [22] revealed that adaphostin synergizes with both vorinostat and entinostat to increase DNA fragmentation in Jurkat and Molt-4 cells as evidenced by combination index (CI) on several combinations, which are less than 1 (Figure 1C). The combinations with the lowest CI values in Jurkat cells range from 0.1 – 0.75 μM adaphostin plus 1 – 0.75 μM vorinostat, and 0.25 – 0.75 μM adaphostin plus 2.5 μM entinostat. The lowest CI values in Molt-4 cells range form 0.5 – 2.5 μM adaphostin plus 1.5 μM vorinostat, and 0.5 – 2.5 μM adaphostin plus 2.5 μM entinostat. These representative synergistic combinations are summarized in Figure 1D, where a combination index (CI) value less than 1.0 indicates synergy.

3.2 Induction of DNA fragmentation by HDACi and adaphostin is caspase-dependent

We next investigated whether a caspase-dependent apoptotic pathway was activated in ALL cells treated with the adaphostin and HDACi combinations. To this end, we measured caspase activity in Jurkat cells using DEVD-amc, a fluorogenic substrate for caspase-3. Jurkat cells treated with 0.5 μM vorinostat or 2.5 μM entinostat did not have a significant increase in caspase-3-like activity. However, adding adaphostin to these HDACi induced more caspase-3-like activity than HDACi as a single agent. The significant increase in caspase-3-like activity was observed starting at 12 hours after treatment (Figure 2A).

When Jurkat cells were exposed to the pan-caspase inhibitor ZVAD for 30 minutes prior to treatment with synergistic combinations of adaphostin and HDACi for 24 hours, DNA fragmentation was completely blocked, confirming that DNA fragmentation by the combination was caspase dependent (Figure 2B). We then used caspase-8, -9 and -3 specific inhibitors to determine what caspases were activated by the synergistic combinations. Interestingly, protection against DNA fragmentation by caspase-3, -8, or -9 inhibitor varied. The caspase-9 inhibitor exerted the strongest protective effect (Figure 2B), suggesting that activation of caspase-9, but not caspase-8, is critical in cell death induced by the combinations. This conclusion was further corroborated by the use of caspase-8 deficient cells. Specifically, caspase-8 deficient Jurkat cells (I9.2) were treated with the single agents alone or in combination, and DNA fragmentation was assessed. Compared to wild-type Jurkat cells, DNA fragmentation in caspase-8 deficient I9.2 cells was only moderately decreased by either adaphostin-vorinostat or the adaphostin-entinostat combinations (Figure 2C), which suggested that cytotoxicity of the combinations does not rely on the expression or activity of caspase-8.

3.3 HDACi and adaphostin combinations disrupt mitochondrial membrane potential and potentiate intracellular superoxide levels

Since caspase-9 inhibition was the most effective at preventing DNA fragmentation induced by the adaphostin and HDACi combinations, we next investigated how the combinations activate caspase-9. Given that caspase-9 can be activated by the intrinsic apoptotic pathway, we decided to measure how the combinations affected mitochondrial membrane potential.

Substantial reduction of mitochondrial membrane potential was detected starting at 12 hours and sustained through 24 hours (Figure 3A), indicating compromised mitochondrial membrane integrity. In addition, pan-caspase inhibition by ZVAD did not block the reduction of membrane potential induced by adaphostin and the HDACi combinations (Figure 3B), suggesting that reduction in mitochondrial membrane potential precedes caspase activation.

Because mitochondria are a major source of endogenous reactive oxygen species (ROS), and reduction of mitochondrial membrane potential is associated with oxidative stress, we hypothesized that ROS would be further enhanced by adaphostin and HDACi combinations as compared to HDACi alone. As shown in Figure 3C, adaphostin potentiated the increase of superoxide (HE) by HDACi (both vorinostat and entinostat), with significant increases occurring at 16 hours and continuing through 24 hours.

3.4 NAC blocks DNA fragmentation in cells treated with adaphostin and vorinostat, but not in cells treated with adaphostin and entinostat

Previous studies have demonstrated that entinostat and vorinostat induce a ROS-dependent cell death [3, 23], and we have shown here that adaphostin potentiates ROS production by these HDACi (Figure 3C). Therefore, we hypothesized that enhanced oxidative stress might contribute to the synergistic induction of DNA fragmentation by adaphostin and HDACi combinations. To test this hypothesis, Jurkat cells were pre-treated with antioxidant N-acetyl-cysteine (NAC) for 30 minutes, and then exposed to adaphostin and HDACi combinations for 24 hours. DNA fragmentation, superoxide levels, mitochondrial membrane potential, and caspase-3 activity were measured. As expected, pre-incubation with NAC blocked the increase of intracellular superoxide levels and prevented the reduction of mitochondrial membrane potential in both combinations (Figure 4A–B). However, caspase-3 activity and DNA fragmentation were reduced by NAC in cells treated with the adaphostin-vorinostat combination, but not in cells treated with the adaphostin-entinostat combination (Figure 4C–D). These contrasting responses to NAC suggested that the mechanism by which the combination of adaphostin-entinostat induced cell death was distinct from the process of adaphostin-vorinostat induced cell death.

3.5 Glutathione (GSH) does not prevent DNA fragmentation and loss of mitochondrial membrane potential in cells treated with adaphostin and HDACi combinations

Oxidative stress occurs when there is an imbalance between reactive oxygen species and cellular antioxidants. Given that NAC predominantly exerts its effects through increasing GSH, the most abundant intracellular antioxidant, we decided to test whether the distinct responses of the combinations to NAC were due to differential handling of GSH. We first measured levels of GSH in Jurkat cells treated with the single agents or drug combinations. We observed a one-fold decrease in GSH in adaphostin-vorinostat group and a two-fold decrease in GSH adaphostin-entinostat group (Figure 5A).

Because the drug combinations differentially affected GSH levels, we then tried to determine whether decrease of GSH is a mechanism by which the drug combinations generate oxidative stress and induce cell death. Jurkat cells were incubated with glutathione

ethyl ester (GSHee), a soluble molecule that is converted to GSH by intracellular esterases for 30 minutes, and mitochondrial membrane potential and DNA fragmentation were measured after single agents or drug combinations treatment. Though GSH levels were increased in cells pre-incubated with GSHee (Figure 5B), the increase in GSH did not block the previously observed loss of mitochondrial membrane potential nor prevent induction of DNA fragmentation (Figure 5C–D). These results suggested that the induction of cell death by the drug combinations was independent of the decrease in GSH since supplying GSH was not preventive of DNA fragmentation.

3.6 HDACi and adaphostin combinations induce differential regulation of oxidative stress related genes

In an effort to broadly investigate the distinct responses to NAC treatment by the two different combinations, we completed a RT-PCR array focused on genes related to oxidative stress and antioxidant defense. Jurkat cells were treated with single agent adaphostin or the two different combinations of adaphostin and HDACi for 8 hours and the resulting gene expression was profiled. Figure 6A shows expression of 89 genes related to oxidative stress and antioxidant defense pathways, and most of the genes profiled were altered by HDACi and adaphostin combinations, indicating the relevance of the pathway in the induction of cell death by the drug combinations. Specifically, aldehyde oxidase 1 (AOX1), glutathione peroxidase-5, and lactoperoxidase (LPO) were all upregulated in cells treated with either of the combinations compared to untreated control cells (Figure 6B–C and Table 1). Glutathione peroxidase 6 (GPX6) and peroxiredoxin 6 (PRDX6) were upregulated in cells treated with the adaphostin-vorinostat combination compared to the adaphostin-entinostat combination, whereas myeloperoxidase (MPO) and angiopoietin-like 7 were down regulated by the adaphostin-vorinostat combination compared to the adaphostin-entinostat combination (Figure 6B–C and Table 1). We also confirmed the upregulation of AOX1 by adaphostin and HDACi combinations using RT-qPCR (Figure 6D). Taken together, these data demonstrate that the ROS-generating compound adaphostin augments HDACi-induced apoptosis in ALL cells via distinct oxidative stress dependent mechanisms in each of the combinations.

4. Discussion

Currently, clinical trials investigating novel approaches to combine HDACi with other classes of anticancer agents are underway for relapsed and refractory acute lymphocytic leukemia patients [25]. The need for rationally designed combinations with HDACi remains high. Despite the known role of HDACi in inducing oxidative stress and apoptosis in leukemia cells [10], little has been reported with regards to augmenting the anti-cancer effects of HDACi by potentiating ROS production pharmacologically. Here, we report that combining HDACi with adaphostin, a ROS generating compound, achieves synergistic induction of cell death, which is caspase dependent and is preceded by compromised mitochondrial integrity. In addition, synergistic cytotoxicity is rescued by the antioxidant NAC in the adaphostin-vorinostat combination but not in the adaphostin-entinostat combination, suggesting distinct mechanisms for ROS generation in response to two different combinations.

Because adaphostin and HDACi may induce cell death through both ROS-independent and dependent mechanisms, we evaluated whether potentiation of ROS accompanied the synergistic increase in apoptosis. Time course analyses revealed that generation of ROS and subsequent mitochondrial membrane depolarization are early events triggered by both adaphostin-vorinostat and adaphostin-entinostat combinations. Similar to our findings, others have reported that entinostat alone [6] or entinostat in combination with the nucleoside analogue fludarabine [26] induces ROS-dependent apoptosis in leukemia cells accompanied by mitochondrial dysfunction. Likewise, Ruefli et al. demonstrated that vorinostat induces ROS-dependent apoptosis of leukemia cells that is accompanied by mitochondrial disruption and cytochrome c release [27].

We further refined the mechanism by demonstrating that the apoptosis initiated by these combinations is caspase-9 and caspase-3 dependent. Our data suggested that adaphostin augments HDACi-induced oxidative stress to promote activation of the stress-initiated intrinsic pathway of apoptosis. Interestingly, Ruefli et al. reported that the ROS-dependent cell death induced by vorinostat in CEM acute leukemia cells is caspase-independent [27]. This discrepancy is likely due to cell specific responses to vorinostat, because others have reported that apoptosis of Jurkat cells induced by vorinostat alone or in combination with the proteasome inhibitor bortezomib is caspase-dependent [28].

We also showed that pretreatment with the antioxidant NAC prevented superoxide accumulation and mitochondrial membrane depolarization by both combinations, indicating that ROS production is necessary for these early steps of apoptosis. Additionally, NAC pretreatment decreased caspase-3 activation and apoptotic DNA fragmentation in cells treated with the adaphostin-vorinostat combination, demonstrating that ROS production is a prerequisite of the synergistic increase in apoptosis rather than a consequence of it.

In contrast to the results in the adaphostin-vorinostat combination, caspase-3 activity and DNA fragmentation were not abrogated by pretreatment with NAC in the adaphostin-entinostat combination, suggesting that vorinostat and entinostat synergize with adaphostin to induce cell death by distinct mechanisms (Figure 7A). While both entinostat and vorinostat alone induce acetylation of histone H3, the combination of adaphostin with these agents did not further augment hyperacetylation (data not shown), further prompting us to focus on alternative mechanisms of synergy such as redox. Since oxidative stress is dependent on the balance of reactive oxygen species and cellular antioxidants we measured changes in glutathione, an important cellular antioxidant. Despite a significant reduction in glutathione levels caused by the adaphostin-entinostat combination, providing the cells with exogenous glutathione did not protect cells from mitochondrial membrane permeabilization, caspase-3 activation, or DNA fragmentation after treatment with either combination. Therefore, the mechanisms by which adaphostin synergizes with these HDACi in Jurkat cells are independent of glutathione.

Interestingly, several genes involved in redox control are differentially regulated by the combinations, which may explain the different responses to NAC. For example, aldehyde oxidase 1 (AOX1), which promotes superoxide generation by oxidizing NADH, is substantially upregulated in the adaphostin-entinostat but not in the adaphostin-vorinostat

combination. AOX1 is a member of the cytosolic molybdenum hydroxylase family and is involved in the metabolism of a wide range of xenobiotic compounds including anti-cancer and immunosuppressive drugs [29, 30]. Recent epigenetic and gene expression profiling studies have identified the association between AOX1 and pathogenesis and progression of several cancers such as prostate, ovarian and brain tumors [31–33]. Interestingly, AOX1 was downregulated due to promoter hypermethylation in a study comparing prostate cancer tissue versus adjacent benign tissue [34]. However, studies so far have not linked AOX1 to histone acetylation. To this end, our results suggested that HDACi may act through promoting the expression of AOX1 to amplify ROS production by adaphostin, thus exerting synergistic induction of cell death (Figure 7B). Another possible mechanism of action may be the induction of ROS by adaphostin can affect how specific HDACi promote redox gene expression. Furthermore, we speculate that the differential upregulation of AOX1 between the adaphostin-entinostat and the adaphostin-vorinostat combination maybe due to specific class of HDAC differentially inhibited by entinostat versus vorinostat. Therefore, specific inhibition of Class I HDACs by entinostat can be linked to specific redox gene expression that leads to robust upregulation of AOX1 expression. Future studies will address these possibilities to elucidate the relevance of AOX1 in adaphostin and HDACi combinations.

Taken together, our results suggest that combining HDACi with ROS generating agents like adaphostin could be a useful strategy to improve the efficacy of HDACi for the treatment of leukemia, however unique redox mechanisms are likely for different HDACi combinations.

Acknowledgments

We are grateful to Phillip Knouse for providing technical support for AOX1 transcript detection.

Funding: Support from NIH (CA115811-S1; P30CA016672 and P50 CA100632) is gratefully acknowledged.

References

1. West AC, Johnstone RW. New and emerging HDAC inhibitors for cancer treatment. J Clin Invest. 2014; 124(1):30–9. [PubMed: 24382387]
2. Masetti R, et al. The role of HDACs inhibitors in childhood and adolescence acute leukemias. Journal of biomedicine & biotechnology. 2011; 2011:148046. [PubMed: 21318168]
3. Dasmahapatra G, et al. The pan-HDAC inhibitor vorinostat potentiates the activity of the proteasome inhibitor carfilzomib in human DLBCL cells in vitro and in vivo. Blood. 115(22):4478–87.
4. Mann BS, et al. FDA approval summary: vorinostat for treatment of advanced primary cutaneous T-cell lymphoma. Oncologist. 2007; 12(10):1247–52. [PubMed: 17962618]
5. Ryan QC, et al. Phase I and pharmacokinetic study of MS-275, a histone deacetylase inhibitor, in patients with advanced and refractory solid tumors or lymphoma. J Clin Oncol. 2005; 23(17):3912–22. [PubMed: 15851766]
6. Rosato RR, Almenara JA, Grant S. The histone deacetylase inhibitor MS-275 promotes differentiation or apoptosis in human leukemia cells through a process regulated by generation of reactive oxygen species and induction of p21CIP1/WAF1 1. Cancer Res. 2003; 63(13):3637–45. [PubMed: 12839953]
7. Gojo I, et al. Phase 1 and pharmacologic study of MS-275, a histone deacetylase inhibitor, in adults with refractory and relapsed acute leukemias. Blood. 2007; 109(7):2781–90. [PubMed: 17179232]
8. Falkenberg KJ, Johnstone RW. Histone deacetylases and their inhibitors in cancer, neurological diseases and immune disorders. Nat Rev Drug Discov. 2014; 13(9):673–91. [PubMed: 25131830]

9. Ceccacci E, Minucci S. Inhibition of histone deacetylases in cancer therapy: lessons from leukaemia. Br J Cancer. 2016; 114(6):605–11. [PubMed: 26908329]
10. Gao S, et al. Potentiation of reactive oxygen species is a marker for synergistic cytotoxicity of MS-275 and 5-azacytidine in leukemic cells. Leuk Res. 2008; 32(5):771–80. [PubMed: 18031811]
11. Chung CG, Poligone B. Cutaneous T cell Lymphoma: an Update on Pathogenesis and Systemic Therapy. Curr Hematol Malig Rep. 2015; 10(4):468–76. [PubMed: 26626770]
12. Thurn KT, et al. Rational therapeutic combinations with histone deacetylase inhibitors for the treatment of cancer. Future Oncol. 2011; 7(2):263–83. [PubMed: 21345145]
13. Kirschbaum M, et al. A phase 1 clinical trial of vorinostat in combination with decitabine in patients with acute myeloid leukaemia or myelodysplastic syndrome. Br J Haematol. 2014; 167(2): 185–93. [PubMed: 25040094]
14. Zhou W, et al. Proteasome inhibitor MG-132 enhances histone deacetylase inhibitor SAHA-induced cell death of chronic myeloid leukemia cells by an ROS-mediated mechanism and downregulation of the Bcr-Abl fusion protein. Oncol Lett. 2015; 10(5):2899–2904. [PubMed: 26722260]
15. Yaseen A, et al. Resveratrol sensitizes acute myelogenous leukemia cells to histone deacetylase inhibitors through reactive oxygen species-mediated activation of the extrinsic apoptotic pathway. Mol Pharmacol. 2012; 82(6):1030–41. [PubMed: 22923501]
16. Nguyen T, et al. HDAC inhibitors potentiate the activity of the BCR/ABL kinase inhibitor KW-2449 in imatinib-sensitive or -resistant BCR/ABL+ leukemia cells in vitro and in vivo. Clin Cancer Res. 2011; 17(10):3219–32. [PubMed: 21474579]
17. Shanafelt TD, et al. Adaphostin-induced apoptosis in CLL B cells is associated with induction of oxidative stress and exhibits synergy with fludarabine. Blood. 2005; 105(5):2099–106. [PubMed: 15388586]
18. Chandra J, et al. Involvement of reactive oxygen species in adaphostin-induced cytotoxicity in human leukemia cells. Blood. 2003; 102(13):4512–9. [PubMed: 12920036]
19. Le SB, et al. Inhibition of mitochondrial respiration as a source of adaphostin-induced reactive oxygen species and cytotoxicity. J Biol Chem. 2007; 282(12):8860–72. [PubMed: 17213201]
20. Fer ND, Shoemaker RH, Monks A. Adaphostin toxicity in a sensitive non-small cell lung cancer model is mediated through Nrf2 signaling and heme oxygenase 1. J Exp Clin Cancer Res. 2010; 29:91. [PubMed: 20618971]
21. Hose C, et al. Transcriptional profiling identifies altered intracellular labile iron homeostasis as a contributing factor to the toxicity of adaphostin: decreased vascular endothelial growth factor secretion is independent of hypoxia-inducible factor-1 regulation. Clin Cancer Res. 2005; 11(17): 6370–81. [PubMed: 16144942]
22. Chou TC, Talalay P. Quantitative analysis of dose-effect relationships: the combined effects of multiple drugs or enzyme inhibitors. Advances in enzyme regulation. 1984; 22:27–55. [PubMed: 6382953]
23. Lucas DM, et al. The histone deacetylase inhibitor MS-275 induces caspase-dependent apoptosis in B-cell chronic lymphocytic leukemia cells. Leukemia. 2004; 18(7):1207–14. [PubMed: 15116122]
24. Long J, et al. Adaphostin cytoxicity in glioblastoma cells is ROS-dependent and is accompanied by upregulation of heme oxygenase-1. Cancer chemotherapy and pharmacology. 2007; 59(4):527–35. [PubMed: 16924499]
25. Bots M, Johnstone RW. Rational combinations using HDAC inhibitors. Clinical cancer research : an official journal of the American Association for Cancer Research. 2009; 15(12):3970–7. [PubMed: 19509171]
26. Rosato RR, et al. Role of histone deacetylase inhibitor-induced reactive oxygen species and DNA damage in LAQ-824/fludarabine antileukemic interactions. Mol Cancer Ther. 2008; 7(10):3285–97. [PubMed: 18852132]
27. Ruefli AA, et al. The histone deacetylase inhibitor and chemotherapeutic agent suberoylanilide hydroxamic acid (SAHA) induces a cell-death pathway characterized by cleavage of Bid and production of reactive oxygen species. Proc Natl Acad Sci U S A. 2001; 98(19):10833–8. [PubMed: 11535817]

28. Zhang F, et al. Sensitization to gamma-irradiation-induced cell cycle arrest and apoptosis by the histone deacetylase inhibitor trichostatin A in non-small cell lung cancer (NSCLC) cells. Cancer Biol Ther. 2009; 8(9):823–31. [PubMed: 19270532]

29. Rivera SP, et al. Identification of aldehyde oxidase 1 and aldehyde oxidase homologue 1 as dioxin-inducible genes. Toxicology. 2005; 207(3):401–9. [PubMed: 15664268]

30. Wright RM, et al. Molecular cloning, refined chromosomal mapping and structural analysis of the human gene encoding aldehyde oxidase (AOX1), a candidate for the ALS2 gene. Redox Rep. 1997; 3(3):135–44. [PubMed: 27406959]

31. Stavrinou P, et al. Expression Profile of Genes Related to Drug Metabolism in Human Brain Tumors. PLoS One. 2015; 10(11):e0143285. [PubMed: 26580399]

32. Park JS, et al. Intraoperative Diagnosis Support Tool for Serous Ovarian Tumors Based on Microarray Data Using Multicategory Machine Learning. Int J Gynecol Cancer. 2016; 26(1):104–13. [PubMed: 26512784]

33. Varisli L. Identification of new genes downregulated in prostate cancer and investigation of their effects on prognosis. Genet Test Mol Biomarkers. 2013; 17(7):562–6. [PubMed: 23621580]

34. Geybels MS, et al. Epigenomic profiling of DNA methylation in paired prostate cancer versus adjacent benign tissue. Prostate. 2015; 75(16):1941–50. [PubMed: 26383847]

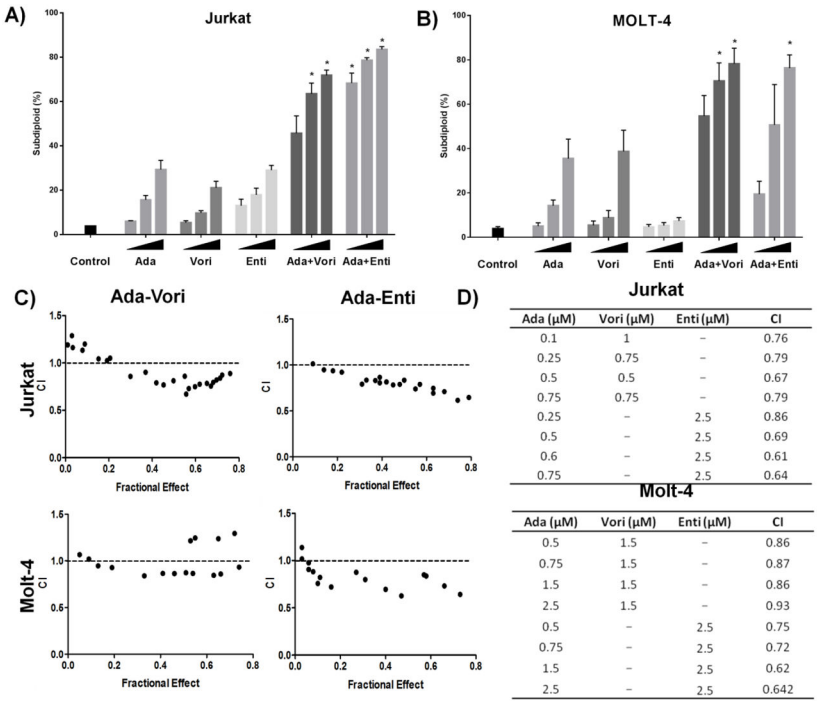

Figure 1. HDACi (vorinostat or entinostat) synergize with adaphostin to induce DNA fragmentation

A) 5×10^5 Jurkat cells and B) Molt-4 were treated with increasing concentrations (0.1–2.5 μM) of adaphostin (Ada), vorinostat (Vori), entinostat (Enti) or the combination of Ada-Vori or Ada-Enti for 24 h. (Single drug concentrations: For Jurkat cells − 0.25, 0.5, and 0.75 μM Ada; 0.25, 0.5, and 0.75 μM Vori; 1, 1.5, and 2.5 μM Enti. For Molt-4 cells − 0.75, 1.5, and 2.5 μM Ada; 0.5, 0.75, and 1.5 μM Vori; 0.75, 1.5, and 2.5 μM Enti). (Drug concentrations in Jurkat cells for: Ada+Vori − 0.25 + 0.75 μM; 0.5 + 0.75 μM and 0.75 + 0.75 μM. Ada +Enti − 0.75 + 1.0 μM; 0.75 + 1.25 μM and 0.75 + 2.5 μM). (Drug concentrations in Molt-4 cells for: Ada+Vori − 0.75 + 1.5 μM; 1.5 + 1.5 μM and 2.5 + 1.5 μM. Ada+Enti − 0.75 + 2.5 μM; 1.5 + 2.5 μM and 2.5 + 2.5 μM). DNA fragmentation (% Subdiploid) was assessed by PI staining using flow cytometry. C) Synergy was calculated using isobologram analysis. A combination index (CI) value < 1.0 indicates synergy. D) Summary of selected synergistic combinations in Jurkat and Molt-4 as indicated by the CI values. Error bars in A& B) represent the means ± S.D. of three independent experiments. *$p < 0.05$ as compared with adaphostin, vorinostat, or entinostat treatment alone.

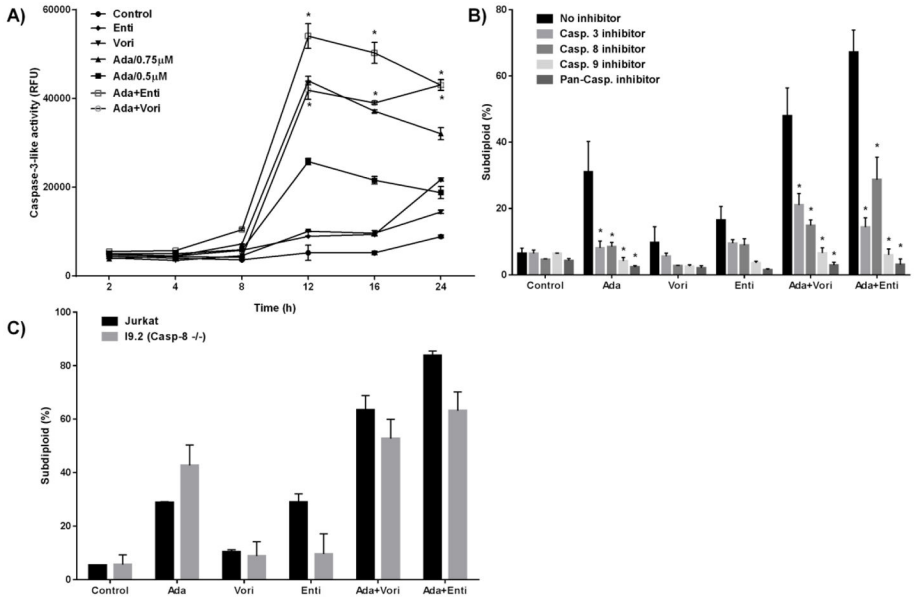

Figure 2. Synergistic induction of DNA fragmentation by adaphostin and HDACi combination is caspase dependent

A) 2×10^6 Jurkat cells were treated with single agents (0.5 μM Vori, 2.5 μM Enti, 0.5 μM Ada, or 0.75 μM Ada), or combinations of 0.5 μM Ada and 0.5 μM Vori or 0.75 μM Ada and 2.5 μM Enti. Caspase-3-like activity was assessed by measuring fluorescence resulting from the cleavage of the fluorogenic substrate DEVD-amc. B) 5×10^5 Jurkat cells were pre-treated with either 20 μM pan-caspase inhibitor, or 25 μM caspase-3, caspase-8, caspase-9 inhibitors for 30 min. Cells were then exposed to 0.5 μM Ada and 0.5 μM Vori or 0.75 μM Ada and 2.5 μM Enti combinations for 24 h. DNA fragmentation was assessed using propidium iodide (PI) staining by flow cytometer. D) & E) 5×10^5 cells, either I9.2 (caspase-8 deficient) or parental Jurkat cells were treated with the combinations of 0.5 μM Ada and 0.5 μM Vori or 0.75 μM Ada and 2.5 μM Enti for 24 h. DNA fragmentation was measured by PI staining. Error bars represent the means ± S.D. of three independent experiments. *$p < 0.05$ as compared with control.

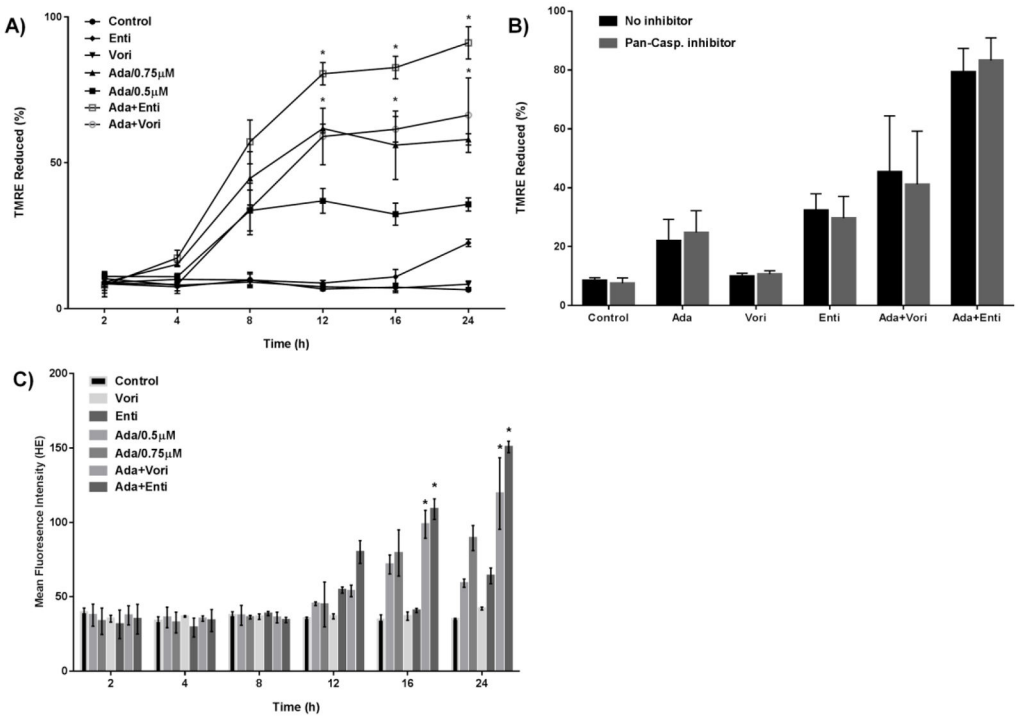

Figure 3. HDACi synergize with adaphostin to increase mitochondrial permeability and superoxide levels

A)5×10^5 Jurkat cells were treated with single agents (0.5 μM Vori, 2.5 μM Enti, 0.5 μM Ada, or 0.75 μM Ada), or combinations of 0.5 μM Ada and 0.5 μM Vori or 0.75 μM Ada and 2.5 μM Enti. Changes in mitochondrial membrane potential were measured by TMRE staining at different time points (2–24 h). B) 5×10^5 Jurkat cells were pre-treated with 20 μM pan-caspase inhibitor for 30 minutes, and then were exposed to above mentioned single agents alone or combinations for 24 h. Mitochondrial membrane potential was measured by TMRE staining. C) 5×10^5 Jurkat cells were treated with above mentioned single agents alone or combinations. Superoxide levels were measured by dHE staining in cells at different time points (2–24 h). Error bars for A–C) represent the means ± S.D. of three independent experiments. *$p < 0.05$ as compared with control.

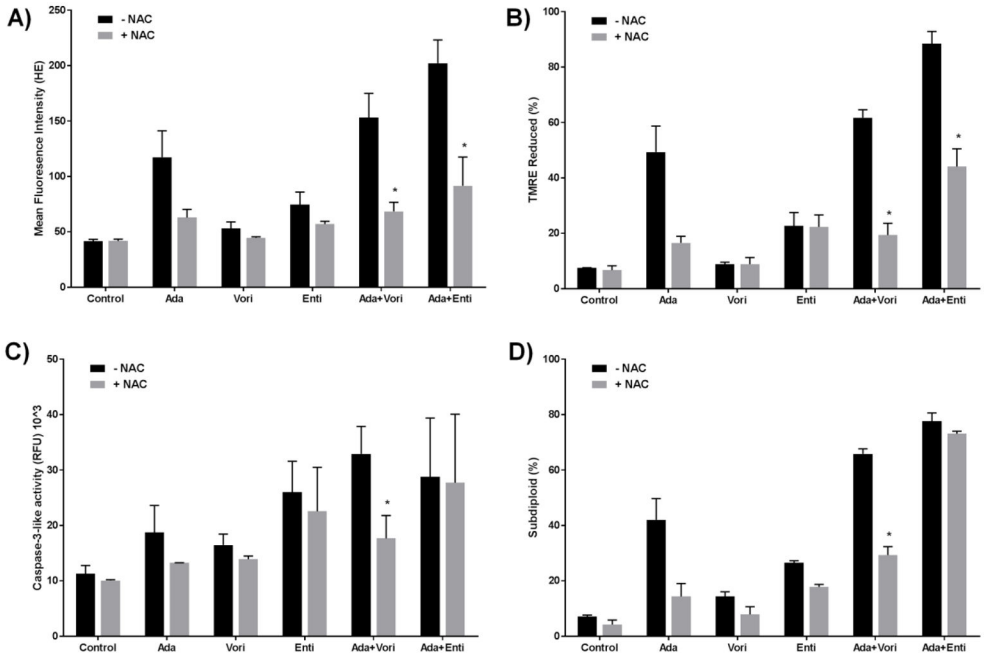

Figure 4. NAC reduces mitochondrial permeability and DNA fragmentation in cells treated with HDACi and adaphostin combinations

Jurkat cells were pre-incubated with 24 mM NAC for 30 min, then treated with single agents (0.5 μM Vori, 2.5 μM Enti, 0.5 μM Ada, or 0.75 μM Ada), or combinations of 0.5 μM Ada and 0.5 μM Vori or 0.75 μM Ada and 2.5 μM Enti for 24 h. 5×10^5 cells were harvested to measure A) Superoxide levels, B) Mitochondrial membrane potential, C) DNA fragmentation and 2×10^6 cells were harvested to measure D) Caspase-3-like activity. Error bars represent the means ± S.D. of three independent experiments. *$p < 0.05$ as compared with no NAC.

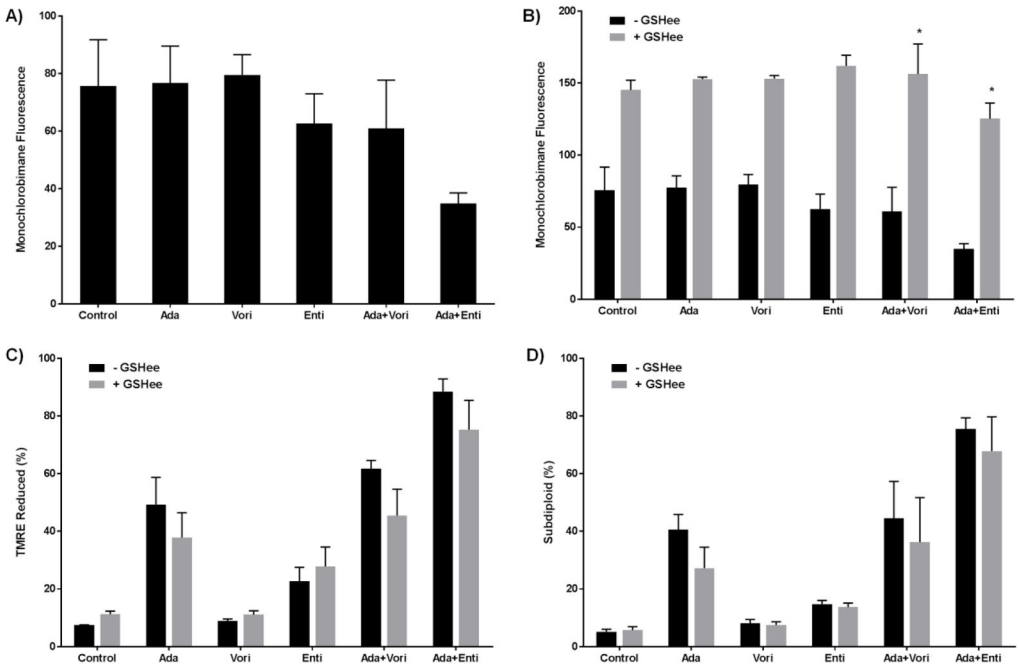

Figure 5. GSHee increases the levels of glutathione (GSH) but does not block the loss of mitochondrial membrane potential or cell death in cells treated with HDACi-Adaphostin

A)1 × 10^6 Jurkat cells were treated single agents (0.5 μM Vori, 2.5 μM Enti, 0.5 μM Ada, or 0.75 μM Ada), or combinations of 0.5 μM Ada and 0.5 μM Vori or 0.75 μM Ada and 2.5 μM Enti for 24 h, and GSH levels were measured using monochlorobimane as a substrate. Jurkat cells were pre-incubated with 1 mM GSHee for 30 min and then treated with the above mentioned single agents or combination for 24 h. 1 × 10^6 cells were harvested to measure B) GSH levels, and 5 × 10^5 cells were harvested to measure C) mitochondrial membrane potential and D) DNA fragmentation. Error bars for all panels represent the means ± S.D. of three independent experiments. *$p < 0.05$ as compared with control.

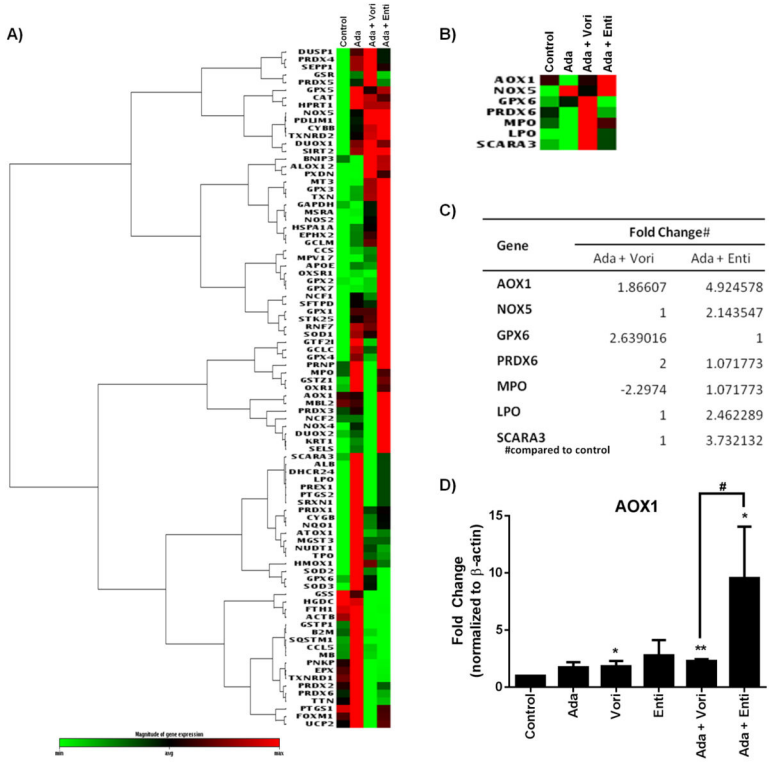

Figure 6. HDACi and adaphostin combinations induce differential regulation of oxidative stress related genes

5×10^6 Jurkat cells were treated 0.75 μM Ada, 0.5 μM Ada and 0.5 μM Vori or 0.75 μM Ada and 2.5 μM Enti combination for 8 h, and samples were harvested for RNA isolation and subjected to oxidative stress and antioxidant defense PCR array analysis. A) Differential expression of 89 genes of interest in the oxidative stress and antioxidant defense PCR array among different treatment conditions were visualized in heatmap using supervised clustering. 7 most differentially expressed genes between Ada-Vori and Ada-Enti combinations were visualized in a separate B) heatmap and fold change of were summarized in C) a table. D) AOX1 expression was confirmed by a separate RT-PCR in jurkat cells treated with single agents (0.5 μM Vori, 2.5 μM Enti, 0.5 μM Ada, or 0.75 μM Ada), or combinations of 0.5 μM Ada and 0.5 μM Vori or 0.75 μM Ada and 2.5 μM Enti for 8 h. Error bars represent the means ± S.D. of three independent experiments. *$p < 0.05$, **$p<0.01$ as compared with control. #$P<0.05$

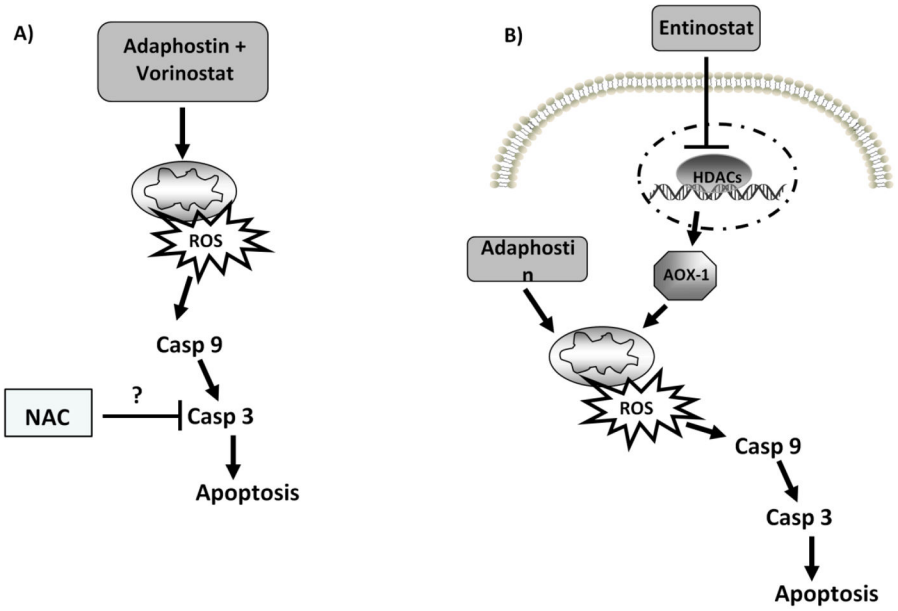

Figure 7. Vorinostat and entinostat synergize with adaphostin to induce apoptosis by distinct mechanisms

Both combinations synergize to promote the activation of the apoptotic intrinsic pathway. Aldehyde oxidase-1 (AOX-1) was upregulated in cells treated with both combinations but at different scale between two combinations. Therefore, it is predicted that ROS production facilitated by AOX-1 is more in entinostat combination than vorinostat combination.

Table 1

Genes involved in oxidative stress are differentially regulated by the Ada-Vori and Ada-Enti combinations

5×10^6 Jurkat cells were treated with the combinations of 0.5 μM Ada and 0.5 μM Vori or 0.75 μM Ada and 2.5 μM Enti for 8 h. Cells were harvested and RT^2 profile PCR array for genes involved in oxidative stress and antioxidant defense was performed. Numbers in red represent gene up-regulation, numbers in blue represent a gene down-regulation and numbers in black represent no change across combinations.

Gene	Ctrl vs. Adaphostin-Vorinostat	Ctrl vs. Adaphostin-Entinostat
Oxidation resistance 1	1.3195	1.6245
Sirtuin 2	1.3195	1
Eosinophil peroxidase	1.3195	
Gluthatione peroxidase 2	1.1487	
Lactoperoxidase	1	
Aldehyde oxidase 1	1.8661	
Gluthatione peroxidase 6		1.1487
Peroxiredoxin 6		1.2311
Chemokine ligand 5		
Gluthatione peroxidase 5		
Thioredoxin reductase 1		
Angiopoietin-like 7		1.6245
Myeloperoxidase		1.2311
Dual oxidase 2		
Epoxide hydrolase		
Prostaglandin-endoperoxide synthase 1		
Glutathione reductase		
Glutathione S-transferase 2		